

The near infrared, visible, and near ultraviolet overtone spectrum of water

M. Carleer, A. Jenouvrier, A.-C. Vandaele, P. F. Bernath, M. F. Mérienne, R. Colin, N. F. Zobov, Oleg L. Polyansky, Jonathan Tennyson, and V. A. Savin

Citation: *The Journal of Chemical Physics* **111**, 2444 (1999); doi: 10.1063/1.479859

View online: <http://dx.doi.org/10.1063/1.479859>

View Table of Contents: <http://scitation.aip.org/content/aip/journal/jcp/111/6?ver=pdfcov>

Published by the [AIP Publishing](#)

Articles you may be interested in

Ultraviolet-visible-near infrared and mid-Fourier transform infrared spectroscopic studies of intermolecular interaction in cholesteryl oleyl carbonate in mesophases

J. Chem. Phys. **124**, 124514 (2006); 10.1063/1.2180782

Direct-potential-fit analysis of new infrared and UV/visible $A \Sigma + 1 - X \Sigma + 1$ emission spectra of AgH and AgD

J. Chem. Phys. **123**, 204304 (2005); 10.1063/1.2064947

High pressure ultraviolet-visible-near infrared study of colored solid hydrogen sulfide

Rev. Sci. Instrum. **73**, 2355 (2002); 10.1063/1.1480455

Response to "Comment on 'The near infrared, visible, and near ultraviolet overtone spectrum of water'" [*J. Chem. Phys.* **112**, 8730 (2000)]

J. Chem. Phys. **112**, 8732 (2000); 10.1063/1.481488

Comment on "The near infrared, visible, and near ultraviolet overtone spectrum of water" [*J. Chem. Phys.* **111**, 2444 (1999)]

J. Chem. Phys. **112**, 8730 (2000); 10.1063/1.481475

An advertisement for AIP Applied Physics Reviews. On the left is a thumbnail image of the journal cover, which features a diagram of a device and the title 'AIP Applied Physics Reviews'. The main background is a blue gradient with a molecular model of a cluster of atoms. The text 'NEW Special Topic Sections' is prominently displayed in white. Below this, in an orange banner, it says 'NOW ONLINE' in yellow, followed by 'Lithium Niobate Properties and Applications: Reviews of Emerging Trends' in white. The AIP Applied Physics Reviews logo is in the bottom right corner.

NEW Special Topic Sections

NOW ONLINE
Lithium Niobate Properties and Applications:
Reviews of Emerging Trends

AIP Applied Physics
Reviews

The near infrared, visible, and near ultraviolet overtone spectrum of water

M. Carleer

Université Libre de Bruxelles, Service de Chimie Physique Moléculaire, CP 160/09, Av. F.D. Roosevelt 50, B-1050 Brussels, Belgium

A. Jenouvrier

Spectrométrie Moléculaire et Atmosphérique, UFR Sciences, Moulin de la Housse, B.P. 1039, 51687 Reims Cedex 2, France

A.-C. Vandaele

Institut d'Aeronomie Spatiale de Belgique, Av. Circulaire 3, B-1180 Brussels, Belgium

P. F. Bernath^{a)}

Department of Chemistry, University of Waterloo, Waterloo, Ontario N2L 3G1, Canada, and Department of Chemistry, University of Arizona, Tucson, Arizona 85721

M. F. Mérienne

Spectrométrie Moléculaire et Atmosphérique, UFR Sciences, Moulin de la Housse, B.P. 1039, 51687 Reims Cedex 2, France

R. Colin

Université Libre de Bruxelles, Service de Chimie Physique Moléculaire, CP 160/09, Av. F. D. Roosevelt 50, B-1050 Brussels, Belgium

N. F. Zobov,^{b)} Oleg L. Polyansky,^{b)} and Jonathan Tennyson

Department of Physics and Astronomy, University College London, London WC1E 6BT, United Kingdom

V. A. Savin

Department of Mathematics, Nizhny Novgorod State University, Nizhny Novgorod, Russia

(Received 6 April 1999; accepted 13 May 1999)

New long path length, high resolution, Fourier transform spectrometer measurements for water are presented. These spectra cover the near infrared, visible, and near ultraviolet regions and contain water transitions belonging to all polyads from 3ν to 8ν . Transitions in the range $13\,100\text{--}21\,400\text{ cm}^{-1}$ are analyzed using line lists computed using variational first-principles calculations. 2286 new transitions are assigned to H_2^{16}O . These result in the observation of transitions in 15 new overtone and combination bands of water. Energy levels for these and other newly observed levels are presented. It is suggested that local mode rather than normal mode vibrational assignments are more appropriate for the vibrational states of water in polyads 4ν and above. © 1999 American Institute of Physics. [S0021-9606(99)00830-2]

I. INTRODUCTION

The spectrum of water in all its phases is of enormous importance in atmospheric science and in astronomy. Solid and liquid water are best detected by characteristic infrared and near infrared absorption bands. For example, solid water ice can be seen in the massive star-forming region in Orion (IRc2) from the ISO satellite.¹ Even from the ground, water ice can be seen in outer solar system bodies such as the moons of the giant planets² and Kuiper belt objects.³ Infrared spectra of clouds in our own atmosphere also show characteristic water ice absorption bands.⁴

The detection of water vapor can be achieved using microwave, far infrared, infrared, and near infrared spectral features. Infrared atmospheric sounders are routinely used from satellites for humidity measurements for weather forecasting purposes.⁵ Water vapor masers are characteristic of star-

forming regions.⁶ Thermal emission spectra of water vapor can also be seen from the ISO satellite in the far infrared and infrared in the Orion nebula.⁷ Extraterrestrial detection of water vapor from the ground is difficult because of atmospheric absorption but hot water can be routinely measured in cool stars,⁸ sunspots,^{9,10} and brown dwarfs.¹¹ After H_2 and CO, water is probably the most abundant molecule in the universe.

In our atmosphere, water is by far the most important greenhouse gas. Astronomical and atmospheric measurements of water usually involve the infrared, far infrared, or microwave regions because the transitions in these regions are strong. Although water can be seen in absorption at wavelengths shorter than $1\text{ }\mu\text{m}$ in, for example, brown dwarfs¹¹ and in our atmosphere, these overtone transitions are weak. It is tempting, therefore, to consider that these water overtones are of minor importance in atmospheric chemistry. Most of the solar flux, however, is emitted in the near UV, visible, and near infrared regions so that the weak water, oxygen, and ozone bands largely control the visible radiation that reaches the surface of the earth.¹² The long

^{a)}Electronic mail: bernath@uwaterloo.ca

^{b)}Permanent address: Institute of Applied Physics, Russian Academy of Science, Uljanov Street 46, Nizhnii Novgorod, Russia 603024.

path length of the solar radiation through our atmosphere partly compensates for the weakness of the visible water bands and makes them important in the earth's radiation balance.

Surprisingly the radiation balance of the earth is still not well understood¹³ in spite of more than a century of research, starting with Arrhenius¹⁴ in 1896. The basic problem is simple to state: the incoming solar flux must be in balance with the outgoing thermal emission in the infrared.¹² This balance has not yet been modeled correctly—even for clear skies where the effects of clouds are minimized. The general consensus is that the atmosphere needs to be about 25% more absorbing in the visible region to achieve this balance. The discrepancy is sometimes called the “missing absorber problem” since some additional absorber needs to be identified.¹³

This lack of balance is a serious embarrassment in atmospheric science. After all, predictions of effects such as global warming involve changes in atmospheric absorption that are typically less than 1% of the total absorption. Various suggestions have been made for resolving this discrepancy. The most popular explanations are related to problems in the calculation of extinction (absorption and scattering) due to clouds. For clear skies, absorption or extinction due to aerosols and thin clouds have been suggested¹³ as the source.

For water vapor, one possibility for the missing absorber lies in the myriad weak lines not currently included in the atmospheric models. Stellar opacity calculations, for example, need to include millions of water lines.¹⁵ It was these atmospheric considerations, as well as problems in interpreting the visible data from the GOME instrument on the ERS-2 satellite,¹⁶ that made us look again at the visible spectrum of water vapor.

We will only consider wavelengths shorter than 1 μm (wave numbers greater than 10 000 cm^{-1}) in our work. The oscillator strength in this region is mainly carried by the O–H stretching vibrations (called ν) which can be combined with bending vibrations (called δ). The bands near 9000 cm^{-1} are thus due to the “ 3ν ” levels. Because two quanta of bend have approximately the same energy as an O–H stretching quantum, the bands in this region include (300), (003), (102), (201), (022), (220), (121), (041), (140), and (060) in the customary normal mode notation. These ten levels can interact with each other to give a very complex spectrum. Of these ten levels, eight are known from the work of Chevillard *et al.*¹⁷ Very recently we have found the (060) level by infrared emission spectroscopy of the (060)–(050) hot band.¹⁸ Further into the visible region the spectroscopy becomes more incomplete as the bands become weaker and more numerous. The $3\nu + \delta$ levels in 11 600–12 800 cm^{-1} have been reexamined by Toth¹⁹ and Flaud *et al.*²⁰ Mandin *et al.*²¹ have measured the 4ν and $4\nu + \delta$ bands between 13 200 and 16 500 cm^{-1} . Finally, Camy-Peyret *et al.*²² have examined the 16 500–25 250 cm^{-1} region for the 5ν , $5\nu + \delta$, 6ν , $6\nu + \delta$, 7ν and 8ν bands.

Many lines remained unassigned in all the spectra until the recent work of Polyansky *et al.*²³ on the 4ν , $4\nu + \delta$ region and Flaud *et al.* on the $3\nu + \delta$ region.²⁰ There are still many unassigned lines in the visible and ultraviolet. Much of

the existing water data is summarized in the HITRAN database,²⁴ and these assignments have been improved and extended by Schwenke.²⁵ The weak water lines show no obvious patterns and traditional methods based on perturbation theory have difficulty in predicting the new energy levels. The recent spate of theoretical work uses new theoretical approaches based either on variational methods,^{10,26} or reformulations of the vibration–rotation Hamiltonian^{20,27,28} to improve convergence.

The visible and near UV spectra of water are in particular need of improvement. The most sensitive experimental techniques for this type of work are based on lasers. Cavity ring down spectroscopy,²⁹ intracavity absorption spectroscopy,³⁰ and frequency modulation spectroscopy³¹ have all been applied to detect weak water lines. These approaches are very sensitive with effective path lengths measured in kilometers but have limited spectral coverage. Direct long-path absorption spectroscopy in the earth's atmosphere is also attractive³² but pressure broadening and pressure shifting of the water lines are a problem. In the work reported here, we use a White multiple reflection cell with a 50 m base path coupled to a high resolution Fourier transform spectrometer in order to record new water spectra from 10 000 to 30 000 cm^{-1} . This experimental approach, combined with the new variationally based theoretical analysis, gives a major improvement in our knowledge of the visible and near visible spectrum of water.

II. EXPERIMENTS

The measurements were carried out using the Bruker IFS 120M high resolution Fourier transform spectrometer of the Laboratoire de Chimie Physique Moléculaire (Université Libre de Bruxelles) coupled to the 50 m base length White-type multiple reflection absorption cell of the Groupe de Spectrométrie Moléculaire et Atmosphérique (Université de Reims). A 450 W xenon arc lamp was used as light source. Two detectors (a Si and a GaP diode) were used to record the spectral region from 10 000 to 30 000 cm^{-1} . The spectra were recorded at room temperature (18 °C). We used 12 traversals through the cell, giving a total absorption path of 602.32 m. This path was chosen because it maximizes the signal-to-noise (S/N) ratio of the recorded spectra. A water pressure of 18.5 hPa was chosen, below the vapor pressure (20.4 hPa) at 18 °C in order to avoid condensation of the water on the mirrors and on the windows. The spectra were recorded at a resolution of 0.06 cm^{-1} (15 cm maximum optical path difference) in two overlapping pieces. In the visible–near infrared region (13 100–22 300 cm^{-1}), the coaddition of some 2048 interferograms in a total recording time of the order of 12 h resulted in a S/N ratio of 3000. In the blue–near ultraviolet part (17 700–30 000 cm^{-1}) of the spectrum, the coaddition of 4096 interferograms (24 h of recording time) proved necessary to attain a S/N ratio of 2500. A third region was recorded in the near infrared (9000–15 000 cm^{-1}) but the lines were mainly saturated. This spectrum contained some weak artifact features caused by the strong lines which interfered with the measurement of weak new features. Spectra in this near infrared region will

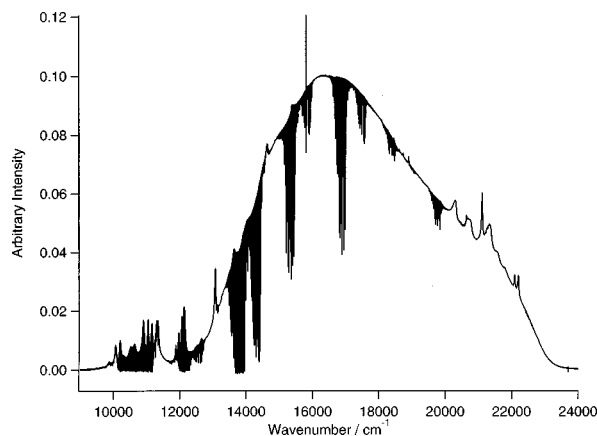


FIG. 1. Overview of the raw measured "visible" spectrum from the near infrared to the near ultraviolet.

be re-recorded in the near future. For each of the three spectral regions discussed above, additional spectra were recorded with nitrogen added in order to determine pressure broadening coefficients. Spectra of "pure" D₂O, and of an equal mixture of H₂O and D₂O were also measured in order to study HOD and D₂O. None of this work will be discussed in this paper. All of the analysis in this first paper is based on the visible-near infrared spectrum of the 13 100–22 300 cm⁻¹ region recorded with the Si photodiode.

III. EXPERIMENTAL RESULTS

An overview of the raw visible–near infrared spectrum is presented as Fig. 1. The overall shape is determined by a blocking filter in the near infrared and the declining response of the Si-photodiode detector in the near ultraviolet. Pressure-broadened Xe atomic emission lines from the lamp give structure to the baseline. The He–Ne laser line can also be seen as an out of phase emission feature at 15 798 cm⁻¹. A more expanded portion of the spectrum is provided in Fig. 2 in order to show the signal-to-noise ratio. Finally, Fig. 3 shows the 8ν region near 25 000 cm⁻¹ (from the blue–near UV spectrum), where the weakest of the observed bands are found.

The line parameters were measured using the SPECTRA program³³ which fitted each feature with a Voigt line shape

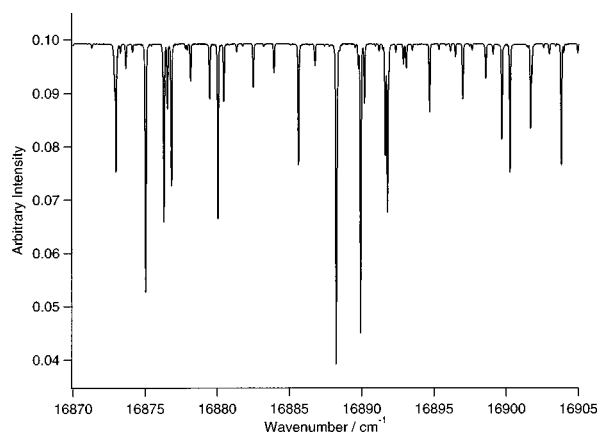


FIG. 2. Expanded part of the experimental spectrum in the visible region.

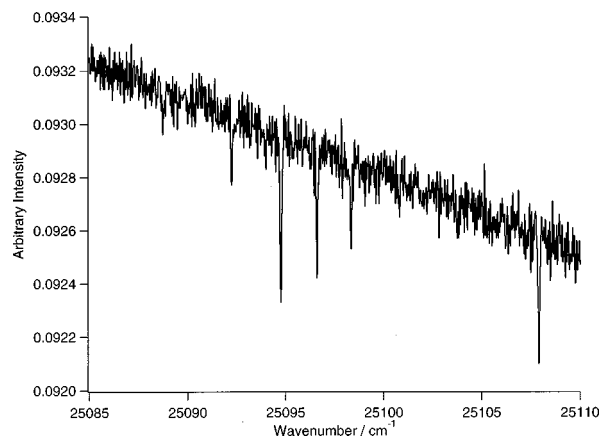


FIG. 3. Expanded part of the experimental spectrum in the near ultraviolet region.

function. In the fitting process, the sinc instrument line shape function was also included but the spectra displayed no "ringing," except for the strongest lines. The advantage of the SPECTRA program is that it also automatically fits the baseline. Because of the long recording times, we could not obtain a reliable spectrum of the empty cell to use as a reference I_0 in the computation of the absorbance. Because we were keen to characterize all the weak lines in the spectrum, some noise spikes were wrongly identified as very weak lines. These spikes can be identified after the fitting procedure because they are unrealistically narrow or broad. We have removed most of these line artifacts from our line list but some remain.

The estimated absolute error in the line positions is 0.004 cm⁻¹. One of the spectra was recorded with an iodine cell placed in the light path. Comparison of the iodine line positions with the values of Gerstenkorn and Luc^{34,35} enabled us to perform a wave number calibration. In the end, the raw spectra were shifted by +0.002 353 cm⁻¹, corrected for the refractive index of air (the spectrometer was not evacuated), and then multiplied by the factor 1.000 001 78. Our calibrated line positions agree with previous work by Camy-Peyret *et al.*²² The output of the SPECTRA program includes for each line a value for the line position (in cm⁻¹), linewidth, line intensity, and approximate equivalent width (line area). For convenience we have included these parameters in our experimental line lists. The line intensity is the natural logarithm absorbance computed from the peak maximum and the local baseline. The units of linewidth and the equivalent width are $\text{mili} \cdot \text{cm}^{-1}$. The equivalent width can be converted to a line intensity in more conventional units, but we have not carried out this conversion. The goal of this paper is the measurement of line positions and the assignment of new lines, as guided by the line intensities. The accurate measurement of line intensities and pressure broadening coefficients has yet to be completed and will be reported elsewhere.

IV. THEORY

The theoretical procedure used to assign the new experimental results follows closely that used by Polyansky *et al.*,²³ who successfully reanalyzed the near infrared spec-

trum of Mandin *et al.*²² This procedure involves the use of calculated linelists. For this we used the same two line lists as Polyansky *et al.*, namely ZVPT³⁶ (Zobov, Viti, Polyansky, and Tennyson) and PS (Partridge and Schwenke).²⁶ These line lists are only for H₂¹⁶O and hence our analysis is restricted to this water isotopomer. We have also measured D₂O and HOD spectra but we will report on this work at a later date.

Both the line lists have been generated using high accuracy variational calculations for the vibration-rotation motion of the water. The major difference between the line lists is that ZVPT is based on *ab initio* calculations with explicit allowance made for non-Born-Oppenheimer effects,³⁷ while the PS line list used a potential which had been refined using spectroscopic data. Along with the two theoretical line lists, we also maintained and updated lists of observed energy levels. The observed energies were used to make further “trivial” assignments and to confirm previous assignments via combination differences. Below we make a distinction between assignments which have been confirmed by combination differences, which can be regarded as secure, and those for which only a single transition involving the upper energy level has been observed, for which occasional misassignments are possible. Over 80% of the assigned transitions reported below have been confirmed by combination differences.

As has been noted before,^{23,38} the PS line list predicts individual transitions with higher accuracy than the ZVPT one, but the errors in the ZVPT are much more systematic, thus allowing trends to be followed for particular classes of transitions. The analysis presented in this work is restricted to transitions up to 21 400 cm⁻¹. The ZVPT line list does not extend beyond this wave number and at wave numbers above 20 000 cm⁻¹, the predictions of the PS line list become increasingly wild. We are in the process of constructing a new, extended *ab initio* line list which will be used to analyze the near ultraviolet region above 21 400 cm⁻¹.

Matching an observed transition with one in the line lists does not automatically give full quantum number assignments to the transition. The ZVPT line list only contains rigorous quantum numbers: for each energy level ZVPT gives (J, p, q) , where J is the rotational angular momentum, p the rotational parity, and q denotes an *ortho* or *para* state. The PS line list gives a full set of quantum numbers but, for the upper states given here, these cannot be relied on.

One reason why the PS quantum numbers are unreliable is because, like all previous spectroscopic studies of water transitions in this region, the vibrational states are labeled using normal modes. However, it is well known that water in the 4ν polyad (and higher) acts as a local mode molecule.^{22,39} See Refs. 40 and 41 for comprehensive reviews of local mode theory. The local mode labels are $(n, m)^\pm \nu_2$, where $n + m = \nu_1 + \nu_3$ and the superscripted sign indicates whether the quanta in each local mode appear as a symmetric or antisymmetric combination. Note that when $n = m$, only the symmetric combination is allowed and the superscripted sign is usually omitted.

In making assignments we found the normal mode labeling increasingly hard to support and we therefore chose to

work within a local mode model. This view is supported by the near degeneracy of the local mode states $(n, 0)^+0$ and $(n, 0)^-0$ for $n=4, 5$, and 6 in the results presented below. The summary tables below label the vibrational states using both notations. However, as noted in the tables, we have switched a considerable number of normal mode assignments used in the original studies^{21,22} to obtain a consistent set of labels for the vibrational states. The more recent theoretical work, e.g., Ref. 42, on water has labels that agree with ours.

V. RESULTS

The complete measured spectrum is too large to list here and therefore has been placed in the E-PAPS electronic archive.⁴³ Tables I and II present summaries of the results. These tables separate the results obtained for 4ν and $4\nu + \delta$, which are presented in Table I, and 5ν , $5\nu + \delta$, 6ν and $6\nu + \delta$ region, which are presented in Table II. These two regions will be discussed separately below.

A. The 4ν and $4\nu + \delta$ polyads

A high resolution spectrum of water vapor in the region 13 200 and 16 400 cm⁻¹ was recorded by Mandin *et al.*²¹ Mandin *et al.* observed 2796 transitions, of which they were able to assign 1927 lines to 17 H₂¹⁶O vibrational bands belonging to the 4ν and $4\nu + \delta$ polyads. A further 51 transitions were ascribed to H₂¹⁸O. Polyansky *et al.*²³ assigned 663 out of the 795 unassigned lines to H₂¹⁶O transitions, including five new vibrational states. They also reassigned 38 lines. Polyansky *et al.* suggested that many of the 132 remaining unassigned lines must be associated with H₂¹⁸O. These results for H₂¹⁶O are summarized in Table I under previous work.

Our measurements yield 3879 lines in the wave number range 13 098–16 397 cm⁻¹. Approximately 35% of these lines are not present in the study of Mandin *et al.* It is these new transitions that we analyze here. So far we have assigned 880 of the new lines to transitions from the ground vibrational state of water and a further 6 transitions to hot bands starting from the (010) vibrational state; 11 lines observed and assigned previously have also been reassigned. Transitions to two vibrational states have been observed for the first time. These are the $(2, 0)^-5$ or (151) state at 14 648 cm⁻¹ and the $(2, 1)^+3$ or (132) state at 15 377 cm⁻¹, where the assignments are in local and normal mode notation, respectively. A full list of assignments are given in the electronic archive⁴³ and are summarized in Table I.

Tables I and II give band origins for the states observed. These band origins were obtained by using two different techniques. A band origin can be obtained accurately and directly if a transition involving the 0₀₀ level of the vibrational state in question is observed. However, if this level is not observed, a less accurate estimate can be obtained by correcting the predicted band origin by the average prediction error of low-lying levels observed in this band. The results of PS were used for this purpose. Band origins determined by the second method are quoted to fewer figures, usually to the nearest 0.1 cm⁻¹.

Besides the two new vibrational states observed, new

TABLE I. Summary of newly assigned transitions in the 13 098–16 397 cm^{-1} range.

Band		Previous (Refs. 21 and 23)		This work			Band origin (cm ⁻¹)
Local mode	Normal mode	Lines	Levels	Lines		Levels	
				a	b		
(2,0) ⁺ 4	240	17	14	12	10	15	13 205.1
(2,0) ⁻ 4	141	56	29	7	8	8	13 256.2
(1,1) 4	042	25	12	1	10	10	13 453.7
(3,0) ⁺ 2	320	109	32	17	5	6	13 640.8
(3,0) ⁻ 2	221	282	95	17	1	1	13 652.656
(1,0) ⁺ 7	170	2	2		3	3	13 661.1
(4,0) ⁺ 0	400 ^c	272	87	21	5	6	13 828.277
(4,0) ⁻ 0	301	376	110	19	6	7	13 830.938
(1,0) ⁻ 7	071	4	3	2			13 835.372
(2,1) ⁺ 2	122	102	52	23	9	11	13 910.896
(2,1) ⁻ 2	023	87	50	9	23	24	14 066.194
(3,1) ⁺ 0	202 ^c	225	82	40	9	13	14 221.161
(3,1) ⁻ 0	103	273	88	53	13	19	14 318.813
(2,2) 0	004	67	41	63	16	30	14 537.505
(2,0) ⁻ 5	151			6	15	18	14 647.978
(3,0) ⁺ 3	330	10	7	9	14	17	15 108.240
(3,0) ⁻ 3	231	108	55	67	11	19	15 119.029
(4,0) ⁺ 1	410 ^d	122	64	42	10	12	15 344.503
(4,0) ⁻ 1	311	225	84	63	8	9	15 347.956
(2,1) ⁺ 3	132			11	11	16	15 377.7
(2,1) ⁻ 3	033	33	26	58	22	37	15 534.709
(3,1) ⁺ 1	212 ^d	44	28	52	17	29	15 742.795
(3,1) ⁻ 1	113	121	61	64	10	17	15 832.765

^aAssignments confirmed by combination differences.^bAssignments made only by comparison with calculated line lists.^cNormal mode assignments swapped.^dNormal mode assignments swapped.

transitions were observed in all previously assigned bands. For four bands, (2,2)⁺0 or (004), (3,0)⁺3 or (330), (2,1)⁻3 or (033), and (3,1)⁺1 or (410), the number of assigned transitions have been approximately doubled. The assignments to the 0₀₀ levels of the (2,2)⁺0 or (004) and (3,0)⁺3 or (330) state means that accurate band origins have been determined for these states for the first time. These accurate band origins are consistent with the predictions of Polyansky *et al.*²³

B. Higher polyads

Camy-Peyret *et al.*²² recorded a high resolution water vapor spectrum in the 16 500–25 250 cm^{-1} region. Nearly all of their lines, 1742 of them, were at wave numbers below the 21 400 cm^{-1} cutoff that we consider here. Camy-Peyret *et al.* assigned 1115 of these lines to 20 H₂¹⁶O vibrational bands belonging to the 5 ν , 5 ν + δ , 6 ν , and 6 ν + δ polyads. Our measurements yield 5146 lines in the same frequency range, approximately three times as many. As we had not previously analyzed Camy-Peyret *et al.*'s spectrum, we combined the analysis of their unassigned lines and our new data. So far we have assigned 1396 new transitions. A further 18 transitions assigned by Camy-Peyret *et al.* were found to be misassigned, and we have so far been able to reassign 15.

This has led to the assignment of 13 new vibrational states and 18 new band origins. These results are summarized in Table II; the full line list containing both assigned and unassigned transitions has been placed in the electronic

archive.⁴³ As shown in the footnotes to Table II, we have relabeled most of the vibrational states assigned by Camy-Peyret *et al.*²² Without this relabeling it is not possible to get a consistent set of local mode labels for the various states. The validity of the local mode designations is shown by the near degeneracy of the pairs of states whose labels differ only by the + or - sign which gives the symmetric or antisymmetric character of the state. This quasidegeneracy is particularly strong for the extreme local mode states ($n,0$)[±]0.

C. Energy levels

One product of the assignment of new spectra is new experimental energy levels for the upper states of the molecule. Because the low-lying states involved in the transitions observed here are known to high accuracy,⁴⁴ one obtains a direct measurement of the excited state level to the accuracy of the experiment. Tables of measured energy levels are useful for a number of applications including the derivation of combination differences as discussed above. As part of our assignment procedure we maintain and update tables of these energy levels.

In this work, our tables (Tables I and II) started from those obtained in previous studies.^{21–23} In the 4 ν and 4 ν + δ polyad region we have added a further 348 levels to the 1022 obtained previously.^{22,23} For the higher polyads, we have more than doubled the number of levels, adding 542

TABLE II. Summary of newly assigned transitions in the 16 400–21 400 cm^{-1} range.

Band		Previous (Ref. 22)		This work			Band origin
Local mode	Normal mode	Lines	Levels	Lines		Levels	(cm $^{-1}$)
				a	b		
(3,0) $^{+4}$	340			33	15	26	16 534.3
(3,0) $^{-4}$	241			42	16	33	16 546.324
(2,1) $^{+4}$	142			76	4	33	16 795.8
(4,0) $^{-2}$	321	131	54	34		3	16 821.635
(4,0) $^{+2}$	420 ^c	39	22	64	9	26	16 823.321
(5,0) $^{+0}$	500 ^d	114	56	66	2	8	16 898.271
(5,0) $^{-0}$	401 ^e	203	76	50			16 898.842
(2,1) $^{-4}$	043			8	8	11	16 967.5
(3,1) $^{+2}$	222 ^c	2	2	38	12	26	17 227.3
(3,1) $^{-2}$	123	53	32	18	2	6	17 312.539
(4,1) $^{+0}$	302 ^d	88	43	48	3	8	17 458.354
(4,1) $^{-0}$	203 ^e	137	57	72		4	17 495.528
(3,2) $^{+0}$	104	5	4	48	25	41	17 748.134
(4,0) $^{-3}$	331	52	28	60	6	22	18 265.819
(4,0) $^{+3}$	430 ^f	2	1	6		3	18 271
(2,1) $^{-5}$	053			18	3	11	18 350.3
(5,0) $^{+1}$	510 ^f	15	7	50	4	27	18 392.974
(5,0) $^{-1}$	411 ^g	62	27	71	2	24	18 393.314
(3,1) $^{-3}$	133			24	13	24	18 758.633
(2,2) $^{-3}$	034			10	3	8	18 977.3
(4,1) $^{-1}$	213 ^g	20	11	66	8	34	18 989.961
(4,0) $^{-4}$	341 ^f	6	4	54	6	32	19 679.196
(2,1) $^{-6}$	063			6		3	19 720
(6,0) $^{-0}$	501 ^h	88	39	59	2	15	19 781.105
(6,0) $^{+0}$	600 ^f	29	17	51	5	18	19 782
(5,0) $^{-2}$	421			19	8	16	19 863
(5,0) $^{+2}$	520			27	1	11	19 864.1
(4,1) $^{-2}$	223			20	5	11	20 441.882
(5,1) $^{+0}$	402			23	15	25	20 533.5
(5,1) $^{-0}$	303 ^h	25	14	32	7	18	20 543.137
(6,0) $^{+1}$	610 ^f	9	6	4	2	4	21 221.569
(6,0) $^{-1}$	511 ^f	25	11	21	1	11	21 221.828
(5,0) $^{-3}$	431			16	2	11	21 312.1

^aAssignments confirmed by combination differences.^bAssignments made only by comparison with calculated line lists.^cNormal mode assignments swapped.^dNormal mode assignments swapped.^eNormal mode assignments swapped.^fNormal mode relabeled.^gNormal mode assignments swapped.^hNormal mode assignments swapped.

new levels to the 511 obtained previously.²¹ A full list of the levels, combining both present and previous results, has been placed in the E-PAPS archive.⁴³

VI. CONCLUSIONS

In this paper we report on new absorption spectra of water obtained over an extended frequency range (13 098–21 400 cm^{-1}). These spectra were recorded using a Fourier transform spectrometer and a long path length cell. A large number of new lines have been recorded. These spectra have been analyzed using line lists computed from variational nuclear motion calculations. 2321 new lines have been assigned and 15 new vibrational states detected. Particularly at higher wave numbers, there remain many transitions which have yet to be assigned. These will be the subject of further analysis.

ACKNOWLEDGEMENTS

The authors acknowledge NATO Grant No. 5–2–05/CRG951293 for making the experimental–theoretical collaboration possible. N. F. Z. thanks the Royal Society for funding visits to University College London. This work was supported by the Prime Minister's Office—Federal Office for Scientific, Technical and Cultural Affairs and the Fonds National de la Recherche Scientifique (Belgium). Support was provided by the Center National de Recherche Scientifique and the Institut National des Sciences de l'Univers through the Program National de Chimie Atmospherique (Contract No. 98N51/0324) (France). The work of O. L. P. was supported in part by the Russian Fund for Fundamental Studies. This work was supported by the Natural Sciences and Engineering Research Council of Canada (NSERC). Acknowledgment is made to the Petroleum Research Fund for partial

support of this work. Some support was also provided by the NASA Laboratory Astrophysics Program, the UK Engineering and Science Research Council, and the UK Natural Environment Research Council.

- ¹E. F. van Dishoeck, C. M. Wright, J. Cernicharo, E. Gonzalez-Alfonso, T. de Graauw, F. P. Helmich, and B. Vandenbussche, *Astrophys. J. Lett.* **502**, L173 (1998).
- ²M. E. Brown, C. D. Koresko, and G. A. Blake, *Astrophys. J. Lett.* **508**, L175 (1998).
- ³M. E. Brown and C. D. Koresko, *Astrophys. J.* **505**, L65 (1998).
- ⁴C. P. Rinsland *et al.*, *J. Quant. Spectrosc. Radiat. Transf.* **60**, 903 (1998).
- ⁵J. T. Houghton, *The Physics of Atmospheres*, 2nd ed. (Cambridge University Press, Cambridge, 1986).
- ⁶J. Cernicharo, R. Bachiller, and E. Gonzalez-Alfonso, *Astron. Astrophys.* **305**, L5 (1996).
- ⁷M. Harwit, D. A. Neufeld, G. J. Melnick, and M. J. Kaufman, *Astrophys. J.* **497**, L105 (1998).
- ⁸K. H. Hinkle and T. G. Barnes, *Astrophys. J.* **227**, 923 (1979).
- ⁹L. Wallace, P. Bernath, W. Livingston, K. Hinkle, J. Busler, B. Guo, and K.-Q. Zhang, *Science* **268**, 1155 (1995).
- ¹⁰O. L. Polyansky, N. F. Zobov, S. Viti, J. Tennyson, P. F. Bernath, and L. Wallace, *Science* **277**, 346 (1997).
- ¹¹C. A. Griffith, R. V. Yelle, and M. S. Marley, *Science* **282**, 2063 (1998).
- ¹²R. P. Wayne, *Chemistry of Atmospheres*, 2nd ed. (Oxford University Press, Oxford, 1991), pp. 40–49.
- ¹³V. Ramanathan and A. M. Vogelmann, *Ambio* **26**, 38 (1997).
- ¹⁴S. Arrhenius, *Philos. Mag.* **41**, 237 (1896).
- ¹⁵F. Allard, P. H. Hauschildt, S. Miller, and J. Tennyson, *Astrophys. J.* **426**, L39 (1994).
- ¹⁶K. V. Chance, J. P. Burrows, D. Perner, and W. Schneider, *J. Quant. Spectrosc. Radiat. Transf.* **57**, 467 (1997); K. Chance (private communication).
- ¹⁷J. P. Chevillard, J.-Y. Mandin, J.-M. Flaud, and C. Camy-Peyret, *Can. J. Phys.* **67**, 1065 (1989).
- ¹⁸N. F. Zobov, O. L. Polyansky, J. Tennyson, J. A. Lotoski, P. Colarusso, K.-Q. Zhang, and P. F. Bernath, *J. Mol. Spectrosc.* **193**, 118 (1999).
- ¹⁹R. A. Toth, *J. Mol. Spectrosc.* **166**, 176 (1994).
- ²⁰J. M. Flaud, C. Camy-Peyret, A. Bykov, O. Naumenko, T. Petrova, A. Scherbakov, and L. Sinista, *J. Mol. Spectrosc.* **183**, 300 (1997); **185**, 211 (1997).
- ²¹J.-Y. Mandin, J.-P. Chevillard, C. Camy-Peyret, J.-M. Flaud, and J. W. Brault, *J. Mol. Spectrosc.* **116**, 167 (1986).
- ²²C. Camy-Peyret, J.-M. Flaud, J.-Y. Mandin, J.-P. Chevillard, J. Brault, D. A. Ramsay, M. Vervloet, and J. Chauville, *J. Mol. Spectrosc.* **113**, 208 (1985).
- ²³O. L. Polyansky, N. F. Zobov, S. Viti, and J. Tennyson, *J. Mol. Spectrosc.* **189**, 291 (1998).
- ²⁴L. S. Rothman *et al.*, *J. Quant. Spectrosc. Radiat. Transf.* **60**, 665 (1998).
- ²⁵D. W. Schwenke, *J. Mol. Spectrosc.* **190**, 397 (1998).
- ²⁶H. Partridge and D. W. Schwenke, *J. Chem. Phys.* **106**, 4618 (1997).
- ²⁷V. I. Starikov and S. Mikhailenko, *J. Mol. Struct.* **449**, 39 (1998).
- ²⁸O. L. Polyansky, *J. Mol. Spectrosc.* **112**, 79 (1985).
- ²⁹J. Xie, B. A. Paldus, E. H. Wahl, J. Martin, T. G. Owano, C. H. Kruger, J. S. Harris, and R. W. Zare, *Chem. Phys. Lett.* **284**, 387 (1998).
- ³⁰B. Kalmar and J. J. O'Brien, *J. Mol. Spectrosc.* **192**, 386 (1998).
- ³¹N. C. Wong and J. L. Hall, *J. Opt. Soc. Am. B* **6**, 2300 (1989).
- ³²J. W. Harder and J. W. Brault, *J. Geophys. Res.* **102**, 6245 (1997).
- ³³M. Carleer, *SPECTRA: A New Program to Measure High Resolution Spectra*, Proceedings of the 12th Symposium on High Resolution Molecular Spectroscopy, Dijon, 1991 (unpublished).
- ³⁴S. Gerstenkorn and P. Luc, *Atlas du Spectre d'absorption de la Molécule d'Iode* (Editions du CNRS, France, 1978).
- ³⁵S. Gerstenkorn and P. Loc, *Rev. Phys. Appl.* **8**, 791 (1979).
- ³⁶O. L. Polyansky, J. Tennyson, and N. F. Zobov, *Spectrochim. Acta A* **55**, 659 (1999).
- ³⁷N. F. Zobov, O. L. Polyansky, C. R. Le Sueur, and J. Tennyson, *Chem. Phys. Lett.* **260**, 381 (1996).
- ³⁸O. L. Polyansky, N. F. Zobov, S. Viti, J. Tennyson, P. F. Bernath, and L. Wallace, *Astrophys. J.* **489**, L205 (1997).
- ³⁹M. S. Child and R. T. Lawton, *Faraday Discuss. Chem. Soc.* **71**, 273 (1981); *Chem. Phys. Lett.* **87**, 217 (1982).
- ⁴⁰M. S. Child and L. Halonen, *Adv. Chem. Phys.* **57**, 1 (1984).
- ⁴¹L. Halonen, *Adv. Chem. Phys.* **104**, 41 (1998).
- ⁴²L. Halonen and T. Carrington, Jr., *J. Chem. Phys.* **88**, 4171 (1988).
- ⁴³See AIP document No. EPAPS: EJCPA6-111-008930 containing the following files: (a) measured spectrum plus assignments in the 13 098–16 397 cm^{-1} range, (b) measured spectrum plus assignments in the 16 400–21 400 cm^{-1} range, and (c) experimental energy levels of H_2^{16}O obtained from this work and previous studies (Refs. 21–23). EPAPS documents may be retrieved free of charge from AIP's FTP server (<http://www.aip.org/pubservs/paps.html>) or from <ftp.aip.org> in the directory /epaps/. For further information, e-mail: paps@aip.org or fax: 516-576-2223.
- ⁴⁴R. A. Toth, *J. Mol. Spectrosc.* **190**, 379 (1998).